

## Eddy Current Testing using the Bode 100

Lukas Heinzle

**Abstract:** Eddy Current Testing (ET) is a commonly used technique for surface inspections of conducting materials. An eddy current sensor, namely a probe coil that produces an alternating electromagnetic field, is placed next to the measurement target (here DUT). Induced eddy currents in the material have an impact on the impedance of the coil. Especially the inductance of the sensor is dependent on the material properties like conductivity and magnetic permeability of the target. By measuring the inductance, it is possible to detect flaws or conductivity variations in the material. This article covers a theoretical calculation and a practical measurement of the sensor-inductance, which is directly measured with the Vector Network Analyzer Bode 100.

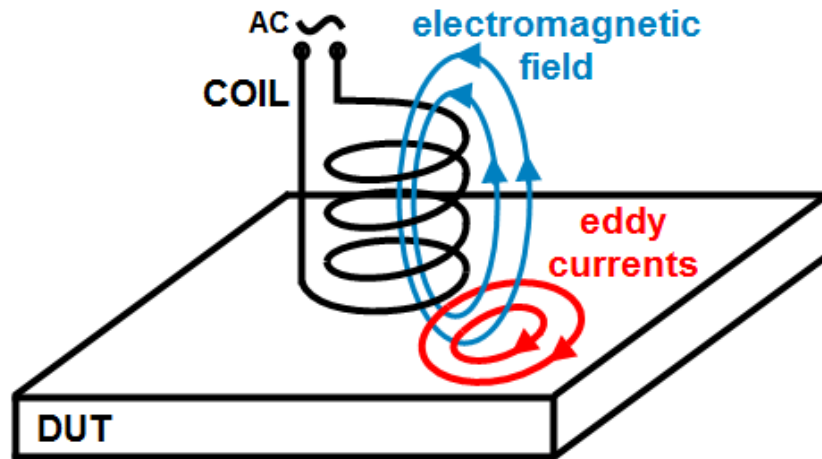


Figure 1: principle of Eddy Current Testing

© 2011 Omicron Lab – V1.1

Visit [www.omicron-lab.com](http://www.omicron-lab.com) for more information.

Contact [support@omicron-lab.com](mailto:support@omicron-lab.com) for technical support.

## Table of Contents

<b>1 Theory of Eddy Currents .....</b>	<b>3</b>
1.1 Concept of a Current Loop.....	3
1.2 Principle of superposition.....	7
1.3 Calculation of the Coil Impedance .....	8
<b>2 Measurement &amp; Results .....</b>	<b>9</b>
2.1 Probe Coil .....	9
2.2 Measurement Targets.....	9
2.3 Setup and Coil Inductance.....	9
2.4 Eddy Current Measurement.....	10
2.5 Conductivity Measurement: .....	11
<b>3 Conclusion .....</b>	<b>12</b>
<b>References.....</b>	<b>12</b>

## 1 Theory of Eddy Currents

The theory of ET is based on classical electromagnetism. An external magnetic field near a conductor according to Faraday's law induces circular currents, so called eddy currents, inside the conductor. Due to these eddy currents, a magnetic field, which by Lenz's law decreases the original magnetic field, is generated. Changing the original magnetic field through the probe coil affects its impedance. The main idea of ET is to measure the variations of the probe coil impedance. Understanding these variations may require some more theory, which is shown in the following section.

### 1.1 Concept of a Current Loop

In order to understand the variations of the impedance, we start with a single-turn coil. The derivation of the impedance of a single-turn coil in this section is based on the approach of Zaman, Long and Gardner<sup>[refA]</sup>. A probe coil can be treated as a superposition of many single-turn coils which is shown in section 1.2. A current loop of radius  $R$  is placed parallel at the height  $h$  above an infinite planar conductor of thickness  $d$  (see figure 2). Moreover we assume the conductivity and magnetic permeability of the conductor to be homogenous and we neglect temperature effects and external electromagnetic fields. The sinusoidal current flowing through the loop can be described as  $I(t) = I_0 e^{i\omega t}$ .

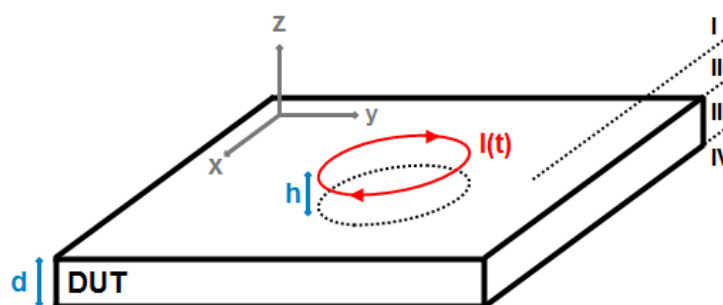


Figure 2: single-turn coil configuration

In our case it is very helpful to use cylindrical coordinates  $(r, \varphi, z)$ . Thus we can write the current density, where  $\delta$  is the Dirac delta function and  $e_\varphi$  is the unit vector in the azimuthal direction.

$$\mathbf{J}(r, \varphi, z, t) = I(t) \delta(z - h) \frac{\delta(r - R)}{r} \mathbf{e}_\varphi \quad (1.1)$$

Due to the low frequency  $f$  of the loop current  $I(t)$  ( $\omega = 2\pi f$ ) we neglect displacement currents. Based on these assumptions, we can write Maxwell's equations in differential form as:

$$\nabla \times \mathbf{H} = \mathbf{J} \quad (1.2)$$

$$\nabla \times \mathbf{E} = -\frac{\partial}{\partial t} \mathbf{B} \quad (1.3)$$

$$\nabla \cdot \mathbf{B} = 0 \quad (1.4)$$

Also recall Ohm's law  $\mathbf{J} = \sigma \mathbf{E}$  and the relation between magnetic induction and magnetic field  $\mathbf{B} = \mu \mathbf{H}$  where  $\sigma$  is the conductivity and  $\mu$  the magnetic permeability. To simplify our calculations, we use the concept of a vector potential<sup>[refB]</sup>  $\mathbf{A}$ .

In particular  $\mathbf{B} = \nabla \times \mathbf{A}$  with the choice of the gauge freedom as  $\nabla \cdot \mathbf{A} = 0$  (Coulomb gauge). This gives us

$$\nabla \times \left( \mathbf{E} + \frac{\partial}{\partial t} \mathbf{A} \right) = 0 \quad (1.5)$$

In general we can write  $\mathbf{E} = -\partial A / \partial t + \nabla \phi$ , where  $\phi$  is an arbitrary scalar potential. Since we are neglecting external electromagnetic fields, we can set  $\phi = 0$  and get

$$\mathbf{E} = -\frac{\partial}{\partial t} \mathbf{A} \quad (1.6)$$

Equation (1.2), also known as Ampere's law, can be written as  $\nabla \times \mathbf{B} = \mu \mathbf{J} = \mu \sigma \mathbf{E}$ . Using the vector identity  $\nabla \times \nabla \times \mathbf{A} = \nabla(\nabla \cdot \mathbf{A}) - \nabla^2 \mathbf{A}$ , we can derive:

$$\nabla^2 \mathbf{A} = \mu \sigma \frac{\partial \mathbf{A}}{\partial t} \quad (1.7)$$

Equation (1.7) is also called diffusion equation. For a none conducting medium we get  $\nabla^2 \mathbf{A} = 0$  because of the conductivity  $\sigma = 0$ . We split our setup into four regions of interest as shown in figure 2, such that we can state the diffusion equation for every region. Note that the vector potential has only an azimuthal component, in particular  $\mathbf{A} = A_\varphi \mathbf{e}_\varphi$ , since  $\mathbf{J}$  is in azimuthal direction.

$$\begin{array}{ll} I & \nabla^2 A_\varphi = \frac{\partial^2 A_\varphi}{\partial r^2} + \frac{1}{r} \frac{\partial A_\varphi}{\partial r} + \frac{\partial^2 A_\varphi}{\partial z^2} - \frac{A_\varphi}{r^2} = 0 \quad \text{for } z > h \\ II & \frac{\partial^2 A_\varphi}{\partial r^2} + \frac{1}{r} \frac{\partial A_\varphi}{\partial r} + \frac{\partial^2 A_\varphi}{\partial z^2} - \frac{A_\varphi}{r^2} = 0 \quad \text{for } 0 < z < h \\ III & \frac{\partial^2 A_\varphi}{\partial r^2} + \frac{1}{r} \frac{\partial A_\varphi}{\partial r} + \frac{\partial^2 A_\varphi}{\partial z^2} - \frac{A_\varphi}{r^2} = i\omega\mu\sigma A_\varphi \quad \text{for } -d < z < 0 \\ IV & \frac{\partial^2 A_\varphi}{\partial r^2} + \frac{1}{r} \frac{\partial A_\varphi}{\partial r} + \frac{\partial^2 A_\varphi}{\partial z^2} - \frac{A_\varphi}{r^2} = 0 \quad \text{for } z < -d \end{array}$$

To solve the equations (I), (II), (III) and (IV) we use the technique of separating variables which yields to a general integral solution. We show this procedure only for equation (III). The other three solutions can be obtained in an analog way. For any  $m \in \mathbb{R}$ ,  $m$  called the separation variable, we can write

$$\frac{\partial^2 A_\varphi}{\partial z^2} - i\omega\mu\sigma A_\varphi = -m^2 A_\varphi \quad (1.8) \quad \text{and} \quad \frac{\partial^2 A_\varphi}{\partial r^2} + \frac{1}{r} \frac{\partial A_\varphi}{\partial r} - \frac{A_\varphi}{r^2} = m^2 A_\varphi \quad (1.9)$$

which is equal to equation (III). Use the separation approach  $A_\varphi = F(r)G(z)$ . Thus it follows from (1.8) and (1.9) that

$$\frac{\partial^2 G}{\partial z^2} + (m^2 + i\omega\mu\sigma)G = 0 \quad (1.10)$$

$$\frac{\partial^2 F}{\partial r^2} + \frac{1}{r} \frac{\partial F}{\partial r} - \left( m^2 + \frac{1}{r^2} \right) F = 0 \quad (1.11)$$

A solution of these equations can be written as

$$G(z) = A(m)e^{\sqrt{m^2 + i\omega\mu\sigma}z} + B(m)e^{-\sqrt{m^2 + i\omega\mu\sigma}z} \quad (1.12)$$

$$F(r) = C(m)J_1(mr) + D(m)N_1(mr) \quad (1.13)$$

Here  $J_1$  is the first-order Bessel function of the first kind,  $N_1$  the first-order Bessel function of the second kind (also called Neumann function) and arbitrary coefficients  $A, B, C, D$ , which are determined by the boundary conditions. The integral solution is

$$A_\varphi = \int_0^\infty [A(m)e^{\sqrt{m^2+i\omega\mu\sigma z}} + B(m)e^{-\sqrt{m^2+i\omega\mu\sigma z}}] \cdot [C(m)J_1(mr) + D(m)N_1(mr)]dm \quad (1.14)$$

A physically realistic situation requires the vector potential  $A_\varphi$  to be limited at the region of interest and to vanish at infinity. Therefore we can say that  $A(m) = 0$  at region I & IV and  $C(m) = 0$  in all regions which leads us to:

$$I' \quad A_{\varphi I} = \int_0^\infty B_I e^{-mz} J_1(mr) dm \quad \text{for } z > h$$

$$II' \quad A_{\varphi II} = \int_0^\infty [A_{II} e^{mz} + B_{II} e^{-mz}] J_1(mr) dm \quad \text{for } 0 < z < h$$

$$III' \quad A_{\varphi III} = \int_0^\infty [A_{III} e^{\sqrt{m^2+i\omega\mu\sigma z}} + B_{III} e^{-\sqrt{m^2+i\omega\mu\sigma z}}] J_1(mr) dm \quad \text{for } -d < z < 0$$

$$IV' \quad A_{\varphi IV} = \int_0^\infty A_{IV} e^{mz} J_1(mr) dm \quad \text{for } z < -d$$

The remaining coefficients are determined by the continuity conditions between the different regions and by the loop current of the coil.

- Continuity of  $A_\varphi$  at  $z = h$ :  $\lim_{z \uparrow h} A_{\varphi I} = \lim_{z \downarrow h} A_{\varphi II}$  gives

$$\int_0^\infty B_I e^{-mh} J_1(mr) dm = \int_0^\infty [A_{II} e^{mh} + B_{II} e^{-mh}] J_1(mr) dm \quad (1.15)$$

Multiply each side by the integral operator  $\int_0^\infty \{...\} J_1(m'r) r dr$  and using the Fourier-Bessel identity (1.16) yields to (1.17):

$$\int_0^\infty J_1(mr) J_1(m'r) r dr = \frac{\delta(m - m')}{m} \quad (1.16)$$

$$B_I e^{-mh} = A_{II} e^{mh} + B_{II} e^{-mh} \quad (1.17)$$

- Due to the loop current, the change of the radial component of the magnetic field is equal to the surface current density of the loop:

$$\lim_{r \uparrow R} H_r - \lim_{r \downarrow R} H_r = \mu I \delta(r - R)$$

Since  $\mathbf{B} = \mu \mathbf{H}$ ,  $\mathbf{B} = \nabla \times \mathbf{A}$  and  $\mathbf{A} = A_\varphi \mathbf{e}_\varphi$  we can get  $H_r = -\frac{\partial A_\varphi}{\partial z}$ , so

$$\left[ -\frac{\partial A_{\varphi I}}{\partial z} + \frac{\partial A_{\varphi II}}{\partial z} \right]_{z=h} = \mu I \delta(r - R) \quad (1.18)$$

$$-B_I e^{-mh} = A_{II} e^{mh} - B_{II} e^{-mh} - \mu I R J_1(mR) \quad (1.19)$$

- At  $z = 0$  and  $z = -d$  we should have a continuous electrical field  $E_\varphi = -i\omega A_\varphi$ :

$$\lim_{z \uparrow 0} E_\varphi = \lim_{z \downarrow 0} E_\varphi \quad \text{and} \quad \lim_{z \uparrow -d} E_\varphi = \lim_{z \downarrow -d} E_\varphi$$

These two boundary conditions lead to:

$$-i\omega \int_0^{\infty} [A_{II} + B_{II}]J_1(mr)dm = -i\omega \int_0^{\infty} [A_{III} + B_{III}]J_1(mr)dm \quad (1.20)$$

$$-i\omega \int_0^{\infty} [A_{III}e^{-\sqrt{m^2+i\omega\mu\sigma}d} + B_{III}e^{\sqrt{m^2+i\omega\mu\sigma}d}]J_1(mr)dm = -i\omega \int_0^{\infty} A_{IV}e^{-md} J_1(mr)dm \quad (1.21)$$

$$A_{II} + B_{II} = A_{III} + B_{III} \quad (1.22)$$

$$A_{III}e^{-\sqrt{m^2+i\omega\mu\sigma}d} + B_{III}e^{\sqrt{m^2+i\omega\mu\sigma}d} = A_{IV}e^{-md} \quad (1.23)$$

- From  $H_r$  continuous at  $z = 0$  and  $z = -d$  we get

$$\lim_{z \uparrow 0} H_r = \lim_{z \downarrow 0} H_r \quad \text{and} \quad \lim_{z \uparrow -d} H_r = \lim_{z \downarrow -d} H_r$$

$$\int_0^{\infty} [mA_{II} \pm mB_{II}]J_1(mr)dm = A_{\phi III} = \int_0^{\infty} \sqrt{m^2 + i\omega\mu\sigma}[A_{III} + B_{III}]J_1(mr)dm \quad (1.24)$$

$$\int_0^{\infty} \sqrt{m^2 + i\omega\mu\sigma} [A_{III}e^{-\sqrt{m^2+i\omega\mu\sigma}d} - B_{III}e^{\sqrt{m^2+i\omega\mu\sigma}d}]J_1(mr)dm = \int_0^{\infty} mA_{IV}e^{-md} J_1(mr)dm \quad (1.25)$$

$$A_{II} - B_{II} = \frac{\sqrt{m^2 + i\omega\mu\sigma}}{m} (A_{III} - B_{III}) \quad (1.26)$$

$$\sqrt{m^2 + i\omega\mu\sigma} [A_{III}e^{-\sqrt{m^2+i\omega\mu\sigma}d} - B_{III}e^{\sqrt{m^2+i\omega\mu\sigma}d}] = mA_{IV}e^{-md} \quad (1.27)$$

As we will see in chapter 1.2, especially region  $I$  is important. Therefore we calculate the coefficient  $B_I$  using equations (1.17, 1.19, 1.22, 1.23, 1.26 and 1.27).

Denote  $\alpha = \frac{\sqrt{m^2+i\omega\mu\sigma}}{m}$  and we can write these six equations as:

$$B_I e^{-mh} = A_{II} e^{mh} + B_{II} e^{-mh} \quad (1.28)$$

$$-B_I e^{-mh} = A_{II} e^{mh} - B_{II} e^{-mh} - \mu I R J_1(mR) \quad (1.29)$$

$$A_{II} + B_{II} = A_{III} + B_{III} \quad (1.30)$$

$$A_{III} e^{-mad} + B_{III} e^{mad} = A_{IV} e^{-md} \quad (1.31)$$

$$A_{II} - B_{II} = \alpha (A_{III} - B_{III}) \quad (1.32)$$

$$\alpha [A_{III} e^{-mad} - B_{III} e^{mad}] = A_{IV} e^{-md} \quad (1.33)$$

$$\alpha [A_{III} e^{-mad} - B_{III} e^{mad}] = A_{III} e^{-mad} + B_{III} e^{mad} \quad (1.34)$$

The next step is to do some algebraic manipulations which stand for themselves.

$$A_{III} = B_{III} e^{2mad} \frac{\alpha + 1}{\alpha - 1}, \quad A_{II} + B_{II} = B_{III} \left[ e^{2mad} \frac{\alpha + 1}{\alpha - 1} + 1 \right], \quad A_{II} - B_{II} = \alpha B_{III} \left[ e^{2mad} \frac{\alpha + 1}{\alpha - 1} - 1 \right]$$

$$(A_{II} - B_{II}) \left[ e^{2mad} \frac{\alpha + 1}{\alpha - 1} + 1 \right] = \alpha (A_{II} + B_{II}) \left[ e^{2mad} \frac{\alpha + 1}{\alpha - 1} - 1 \right]$$

$$(A_{II} - B_{II}) [e^{2mad} (\alpha + 1) + \alpha - 1] = \alpha (A_{II} + B_{II}) [e^{2mad} (\alpha + 1) - \alpha + 1]$$

$$A_{II} \left[ e^{2mad} (\alpha + 1) + \alpha - 1 - \alpha [e^{2mad} (\alpha + 1) - \alpha + 1] \right]$$

$$= B_{II} \left[ \alpha [e^{2mad} (\alpha + 1) - \alpha + 1] + [e^{2mad} (\alpha + 1) + \alpha - 1] \right]$$

$$A_{II} = B_{II} \frac{[\alpha e^{2mad} (\alpha + 1) - \alpha^2 + \alpha + e^{2mad} (\alpha + 1) + \alpha - 1]}{[e^{2mad} (\alpha + 1) + \alpha - 1 - \alpha e^{2mad} (\alpha + 1) + \alpha^2 - \alpha]}$$

$$A_{II} = B_{II} \frac{[e^{2mad}(\alpha + 1)^2 - (\alpha - 1)^2]}{[-e^{2mad}(\alpha^2 - 1) + (\alpha^2 - 1)]}$$

$$B_{II} = A_{II} \frac{(\alpha^2 - 1)[1 - e^{2mad}]}{[e^{2mad}(\alpha + 1)^2 - (\alpha - 1)^2]}$$

$$-A_{II}e^{mh} - B_{II}e^{-mh} = A_{II}e^{mh} - B_{II}e^{-mh} - \mu I R J_1(mR)$$

$$A_{II} = e^{-mh} \frac{\mu I R J_1(mR)}{2} \quad B_{II} = A_{II}e^{2mh} + B_{II}$$

$$B_I = e^{mh} \frac{\mu I R J_1(mR)}{2} + e^{-mh} \frac{\mu I R J_1(mR)}{2} \frac{(\alpha^2 - 1)[1 - e^{2mad}]}{[e^{2mad}(\alpha + 1)^2 - (\alpha - 1)^2]}$$

$$B_I = e^{-mh} \frac{\mu I R J_1(mR)}{2} \left[ e^{2mh} + \frac{(\alpha^2 - 1)[1 - e^{2mad}]}{[e^{2mad}(\alpha + 1)^2 - (\alpha - 1)^2]} \right]$$

A solution to the vector potential in region I is then

$$A_{\phi I} = \frac{\mu I R}{2} \int_0^\infty J_1(mR) J_1(mr) e^{-m(z+h)} \left[ e^{2mh} + \frac{(\alpha^2 - 1)[1 - e^{2mad}]}{[e^{2mad}(\alpha + 1)^2 - (\alpha - 1)^2]} \right] dm \quad (1.35)$$

If we assume that there is no conductor next to the coil, i.e. conductivity  $\sigma = 0$  or thickness  $d = 0$ , we can set  $\alpha \equiv 1$ . The second term in the integral vanishes and thus the first term represents the inductance of the coil in free space. In general, this first term does not converge and thus we only focus on the change in the vector potential  $\delta A_{\phi I}$  due to a DUT as:

$$\delta A_{\phi I}(r, z, R, h) = \frac{\mu I R}{2} \int_0^\infty J_1(mR) J_1(mr) e^{-m(z+h)} \left[ \frac{(\alpha^2 - 1)[1 - e^{2mad}]}{[e^{2mad}(\alpha + 1)^2 - (\alpha - 1)^2]} \right] dm \quad (1.36)$$

## 1.2 Principle of superposition

Until now we assumed that the current is flowing around a single-turn coil. In the practical situation we have N windings in several layers as shown in Figure 3. By neglecting the coil skin-effects we can mathematically describe such a configuration with the superposition principle of a sufficiently high number of single-turn coils. This is a valid assumption since Maxwell's equations are linear.

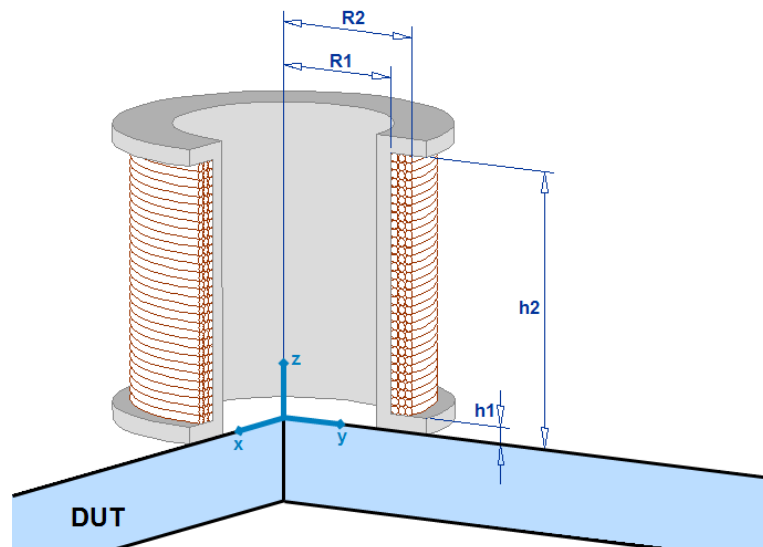


Figure 3: cross-section of the probe coil configuration

By superposing single-turn coils we can derive the total change in the vector potential in region  $I$ :

$$\delta A_{\phi total}(r, z) = \sum_{R, h} \delta A_{\phi l}(r, z, R, h) \quad (1.37)$$

Note that  $R$  and  $h$  have discrete values  $R \in \{R1, \dots, R2\}$  and  $h \in \{h1, \dots, h2\}$ . The steps between  $\{R1, \dots, R2\}$  and  $\{h1, \dots, h2\}$  only depend on the number of windings  $N$  and the dimensions of the housing. All other parameters such as  $\mu$ ,  $\sigma$ ,  $d$  are assumed to be constant.

### 1.3 Calculation of the Coil Impedance

So far we have described the change of the vector potential due to eddy currents. We will first calculate the impedance of a single-turn coil and extend it for the superposed solution. The impedance of a single-turn coil is defined by  $Z = U/I$  where  $U$  is the potential difference and  $I$  the current flowing through the coil. According to Faraday's law, a change of the magnetic induction  $B$  through a single-turn coil<sup>1</sup> placed at height  $h'$  and radius  $R'$  produces an e.m.f.<sup>2</sup> which leads to a change of the potential  $\delta U$ . Namely

$$\delta U = \frac{d}{dt} \int_C \delta \mathbf{B} \cdot d\mathbf{a} \quad (1.38)$$

Using the vector potential  $\mathbf{A}$  and Stokes's theorem from vector calculus we can derive

$$\delta U = \frac{d}{dt} \int_C (\nabla \times \delta \mathbf{A}) \cdot d\mathbf{a} = \frac{d}{dt} \oint_{\partial C} \mathbf{A} \cdot d\mathbf{l} = \oint_{\partial C} \frac{\partial}{\partial t} \mathbf{A} \cdot d\mathbf{l} = j\omega A_{\phi total}(R', h') 2\pi R' \quad (1.39)$$

Hence the change of impedance for a single-turn coil at height  $h$  and radius  $R$  is:

$$\delta Z = i\omega \frac{2\pi R'}{I} A_{\phi total}(R', h') \quad (1.40)$$

The total impedance of the coil is:

$$\delta Z_{total} = \sum_{R', h'} \delta Z(R', h') \quad (1.41)$$

Again,  $R'$  and  $h'$  have discrete values  $R' \in \{R1, \dots, R2\}$  and  $h' \in \{h1, \dots, h2\}$ . Now we are able to write a compact solution to the change of impedance due to eddy currents.

$$\delta Z_{total} = \sum_{R', h'} i\omega 2\pi R' \sum_{R, h} \frac{\mu R}{2} \int_0^{\infty} J_1(mR) J_1(mR') e^{-m(h'+h)} \left[ \frac{(\alpha^2 - 1)[1 - e^{2mad}]}{[e^{2mad}(\alpha + 1)^2 - (\alpha - 1)^2]} \right] dm \quad (1.42)$$

A special interest lies on the coil inductance which is defined as

$$L = \frac{Im(Z)}{\omega} \quad (1.43)$$

Which leads us to a closed form of the change of inductance

$$\partial L = Im \left[ \sum_{R', h'} \sum_{R, h} i\pi \mu R' R \int_0^{\infty} J_1(mR) J_1(mR') e^{-m(h'+h)} \left[ \frac{(\alpha^2 - 1)[1 - e^{2mad}]}{[e^{2mad}(\alpha + 1)^2 - (\alpha - 1)^2]} \right] dm \right] \quad (1.44)$$

<sup>1</sup> Denote  $C$  as the area contained in the loop and  $\partial C$  as the boundary

<sup>2</sup> Electromotive force (Faraday's law)

## 2 Measurement & Results

### 2.1 Probe Coil

For the practical measurements we use a probe coil (figure 4) similar to the one in figure 3, which is soldered to a BNC plug. Technical data:

- R1=6 mm
- R2=7.4 mm
- H1=0.4 mm
- H2=9.6 mm
- Windings per layer: 25
- Number of layers: 4
- Total windings: 100
- Strand: copper,  $\varnothing$  0.35 mm



Figure 4: probe coil

### 2.2 Measurement Targets

We will use two conducting plates (length  $\gg$  probe coil diameter) as DUTs with the following properties:

- Thickness  $d = 1$  mm (both)
- Aluminum  $\mu = 1.256 \times 10^{-6}$  H/m  $\sigma = 3.5 \times 10^7$  S/m
- Copper  $\mu = 1.256 \times 10^{-6}$  H/m  $\sigma = 5.86 \times 10^7$  S/m



Figure 5: aluminum plate



Figure 6: copper plate

### 2.3 Setup and Coil Inductance

First of all we have to set up the internal configuration of the Bode 100.

Measurement:	Frequency Sweep Mode, Impedance
Start Frequency:	100 Hz
Stop Frequency:	100 kHz
Sweep Mode:	Logarithmic
Number of Points:	401 or more
Receiver Bandwidth:	100 Hz or lower
Level:	13 dBm

After the internal setup is done, we perform a user calibration in the impedance mode. Now it is possible to measure the inductance of the probe coil in free space<sup>3</sup>.

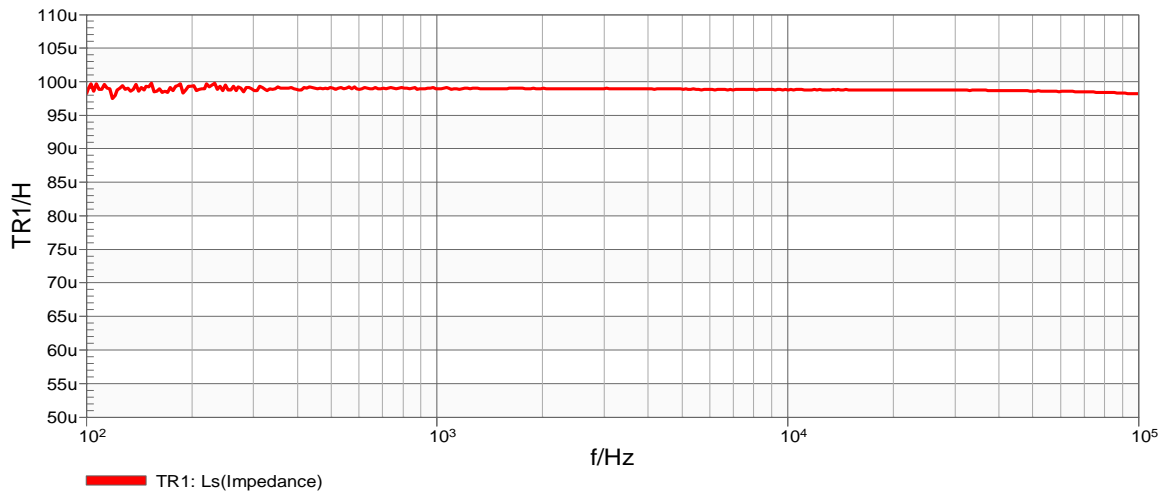


Figure 7: free space inductance

The probe coil inductance has almost a constant value of 99μH over the measurement frequency range.

## 2.4 Eddy Current Measurement

To show that the theoretical prediction obtained in chapter 1 agrees with the practical measurement for an aluminum plate with a thickness of 1 mm, we have to calculate the change of inductance. Therefore we evaluate expression (1.44) numerically. Since the integrand factors go towards zero, the influence of them can be neglected for values of  $m > 10^4$ . The inductance of the probe coil can then be expressed as

$$L \approx 99\mu H + Im \left[ \sum_{R',h'} \sum_{R,h} i\pi\mu R'R \int_0^{10^4} J_1(mR)J_1(mR')e^{-m(h'+h)} \left[ \frac{(\alpha^2 - 1)[1 - e^{2mad}]}{[e^{2mad}(\alpha + 1)^2 - (\alpha - 1)^2]} \right] dm \right]$$

with  $R, R' \in \{6.00, 6.35, 6.70, 7.05, 7.40\}$  mm and  $h, h' \in \{0.4, 0.75, 1.00, \dots, 9.25, 9.60\}$  mm. We have set up the Bode 100 as described in section 2.3 and place the probe coil above the aluminum and copper DUT as shown in figure 8.



Figure 8: eddy current measurement

<sup>3</sup> No metal conductors near to the probe

This leads to a change in the inductance of the probe coil.

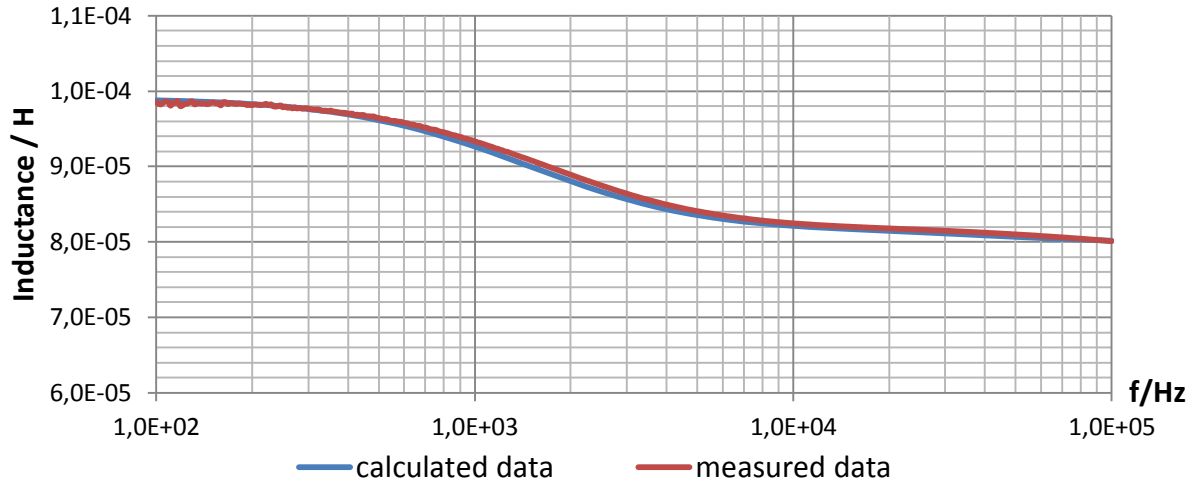


Figure 9: aluminum DUT

frequency [Hz]		1.00E+02	5.00E+02	1.00E+03	5.00E+03	1.00E+04	5.00E+04	1.00E+05
aluminum	calc. inductance [H]	9.88E-05	9.62E-05	9.27E-05	8.36E-05	8.21E-05	8.07E-05	8.02E-05
	meas. inductance [H]	9.85E-05	9.64E-05	9.34E-05	8.41E-05	8.25E-05	8.10E-05	8.01E-05
	rel. error [%]	<b>0.25%</b>	<b>0.28%</b>	<b>0.75%</b>	<b>0.63%</b>	<b>0.40%</b>	<b>0.41%</b>	<b>0.09%</b>
copper	calc. inductance [H]	9.85E-05	9.36E-05	8.91E-05	8.24E-05	8.16E-05	8.03E-05	7.99E-05
	meas. inductance [H]	9.86E-05	9.45E-05	9.02E-05	8.24E-05	8.15E-05	8.01E-05	7.93E-05
	rel. error [%]	<b>0.19%</b>	<b>0.93%</b>	<b>1.18%</b>	<b>0.06%</b>	<b>0.12%</b>	<b>0.15%</b>	<b>0.70%</b>

Table 1: comparison of the calculated and measured impedance

## 2.5 Conductivity Measurement:

The idea of the conductivity measurement is to distinguish between the conductivity of different materials. The result can be used to detect surface flaws or material oxidations. To demonstrate the influence of the conductivity we will show the difference of copper and aluminum. Therefore we place the probe coil above the aluminum and copper DUT as shown in figure 8 and measure the inductance. Here the memory trace represents the aluminum and the data trace the copper plate.

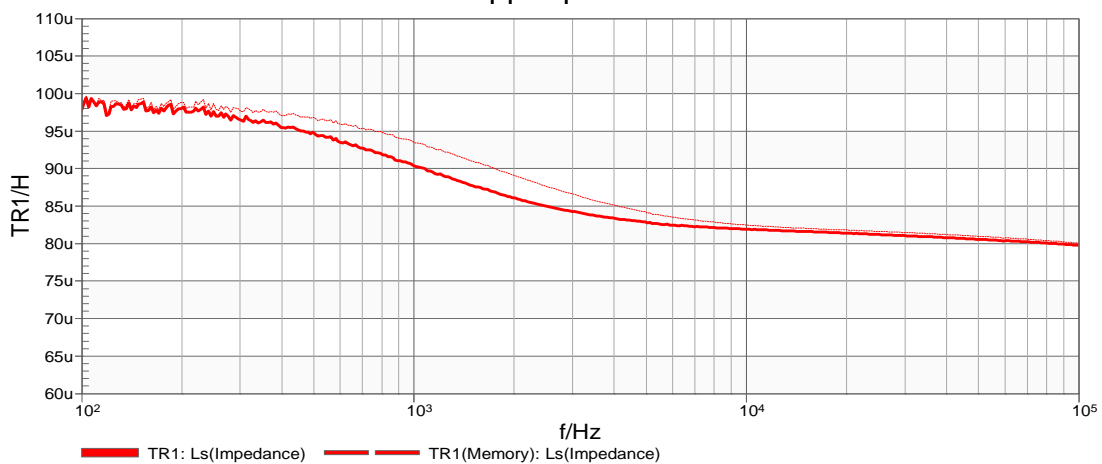


Figure 10: aluminum and copper DUT (both measured)

The same numerical evaluation as in section 2.4 gives us the following theoretical prediction.

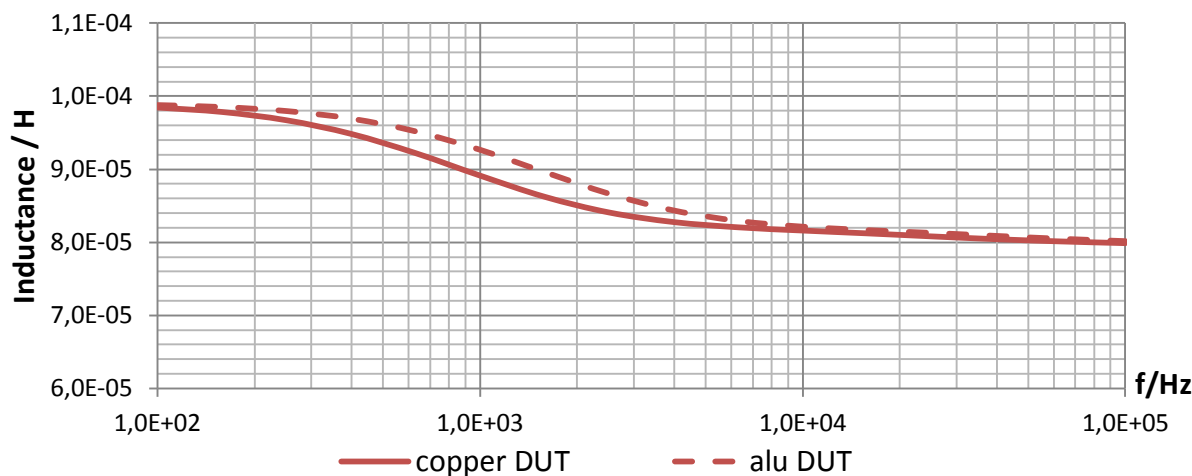


Figure 11: aluminum and copper DUT (both calculated)

Finally we can compare the calculated and measured inductances of the probe coil.

frequency [Hz]	1.00E+02	5.00E+02	1.00E+03	5.00E+03	1.00E+04	5.00E+04	1.00E+05	
aluminum vs. copper	calc. difference [H]	3.32E-07	2.54E-06	3.53E-06	1.19E-06	5.29E-07	4.09E-07	2.79E-07
	meas. difference [H]	1.09E-07	1.94E-06	3.18E-06	1.67E-06	9.56E-07	8.59E-07	7.67E-07
	rel. calc. diff. [%]	<b>0.34%</b>	<b>2.64%</b>	<b>3.81%</b>	<b>1.42%</b>	<b>0.64%</b>	<b>0.51%</b>	<b>0.35%</b>
	rel. meas. diff. [%]	<b>0.11%</b>	<b>2.01%</b>	<b>3.40%</b>	<b>1.98%</b>	<b>1.16%</b>	<b>1.06%</b>	<b>0.96%</b>

Table 2: calculation and measurement data

### 3 Conclusion

In chapter 1 we have shown a theoretical calculation of the probe coil impedance based on classical electrodynamics. The main concept was using the superposition principle which allowed us to simplify the problem to a single-turn coil. Based on the calculations in chapter 1 we have numerically evaluated the impedance of the probe coil. The practical measurement with the Vector Network Analyzer Bode 100 verified the theoretical approach as shown in Figure 9 and Table 1. As explained in the introduction, ET is often used to detect flaws in conducting materials. A theoretical treatment of such flaws is very difficult, sometimes impossible. In order to show how the conductivity of the used DUT influences the probe coil inductance, we have compared a copper with an aluminum plate. Again the measurement results, as stated in Figure 11 and Table 2, match well with the theoretical prediction.

### References

[refA].....J.M. Zaman, Stuart A. Long and C. Gerald Gardner: The Impedance of a Single-Turn Coil Near a Conducting Half Space, *Journal of Nondestructive Evaluation*, Vol. I, No. 3, 1980

[refB].....J.D. Jackson: *Classical Electrodynamics*, 3rd edition, Wiley (1999), p.218-219